Structural features of the ε subunit of the *Escherichia coli* ATP synthase determined by NMR spectroscopy

Stephan Wilkens[1], Frederick W. Dahlquist[1], Lawrence P. McIntosh[2], Logan W. Donaldson[2] and Roderick A. Capaldi[1]

The tertiary fold of the ε subunit of the *Escherichia coli* F_1F_0 ATPsynthase (ECF_1F_0) has been determined by two- and three-dimensional heteronuclear (^{13}C, ^{15}N) NMR spectroscopy. The ε subunit exhibits a distinct two domain structure, with the N-terminal 84 residues of the protein forming a 10-stranded β-structure, and with the C-terminal 48 amino acids arranged as two α-helices running antiparallel to one another (two helix hairpin). The β-domain folds as a β-sandwich with a hydrophobic interior between the two layers of the sandwich. The C-terminal two-helix hairpin folds back to the N-terminal domain and interacts with one side of the β-domain. The arrangement of the ε subunit in the intact F_1F_0 ATP synthase involves interaction of the two helix hairpin with the F_1 part, and binding of the open side of the β-sandwich to the *c* subunits of the membrane-embedded F_0 part.

[1]Institute of Molecular Biology, University of Oregon, Eugene, Oregon 97401, USA
[2]Department of Biochemistry and Molecular Biology and Department of Chemistry, University of British Columbia, Vancouver, British Columbia V6T 1Z3, Canada

Correspondence should be addressed to R.A.C.

A proton-pumping ATPase, found in the plasma membrane of bacteria, the inner membrane of mitochondria and the thylakoid membrane of chloroplasts, acts both to synthesize ATP driven by an electrochemical gradient and to hydrolyze ATP coupled with proton translocation across the membrane. This complex enzyme is made up of two parts: an F_1 part composed of five different subunits α,β,γ,δ and ε in the molar ratio 3:3:1:1:1 and an F_0 sector, which in the bacterial enzyme ECF_1F_0 contains subunits a, b and c in the ratio 1:2:9–12 (for recent reviews, see refs 1–3).

Electron microscopy[4,5], in conjunction with the recently published X-ray determination of the F_1 part[6], provides a picture of the F_1F_0 complex in which the three α and β subunits are arranged as a hexagon around a central cavity within which is located a part of the γ subunit. The γ subunit extends from the bottom of F_1 into a narrow stalk region 40–45 Å long that separates the F_1 and membrane-embedded F_0 parts. Binding of the F_1 part to the membrane-bound F_0 part requires both the δ and the ε subunits[7,8] indicating that these two subunits, in addition to the γ subunit, are involved in forming the stalk.

Catalytic-site events (ATP synthesis and ATP hydrolysis in sites on the β subunits) appear to be linked to proton translocation through conformational changes in the stalk-forming subunits. There is evidence from proteinase digestion studies[9,10], fluorescence measurements[11], cross-linking[12] and electron microscopy studies[13,14] that the ε subunit changes conformation and/or moves between different sites in the ECF_1F_0 complex during enzyme functioning. These important observations could be better understood if the structure of the ε subunit and its location(s) in the F_1F_0 complex were known. Unfortunately in the two crystal forms of F_1 examined to date, from beef heart mitochondria[6] (MF_1) and rat liver mitochondria[16], the homologue of the ε subunit of the bacterial and chloroplast enzyme is disordered. Here we describe structural studies of the isolated ε subunit for the *E. coli* F_1-ATPase in solution using nuclear magnetic resonance spectroscopy. The secondary structure and global fold of the ε subunit, in conjunction with biochemical studies, provides information on the arrangement of this polypeptide in the ECF_1F_0 complex.

Secondary structure

Amino-acid type-specific assignments were obtained by a combined strategy of selective labelling with ^{15}N-amino acids and 3D ^{15}N-TOCSY-HSMQC experiments. Approximately 50% of the backbone amide resonances were readily assigned by isotopic labelling with ^{15}N-alanine, valine, leucine, isoleucine or glutamic acid. The majority of the remaining spin systems were assigned from a 3D ^{15}N-TOCSY-HSMQC experiment. Initially 10 amino acids (besides the four prolines and the first two N-terminal residues) were not identified in any ^{15}N-^{1}H correlation spectrum recorded with presaturation for water suppression. This is due to the relatively high pH (7.4) and low protein concentration (0.6–1 mM) necessary to keep the protein from aggregating.

Sequence-specific residue assignments of the backbone amide resonances were obtained from 3D ^{15}N-NOESY-HSMQC and 3D H(CCO)TOCSY-NH experiments. All but one (Tyr 35) of the 10 missing amide resonances could be identified in the H(CCO)TOCSY-NH experiment due to the use of flip-back pulses and pulsed field gradients to minimize perturbation of the magnetization of water. ^{13}C reso-

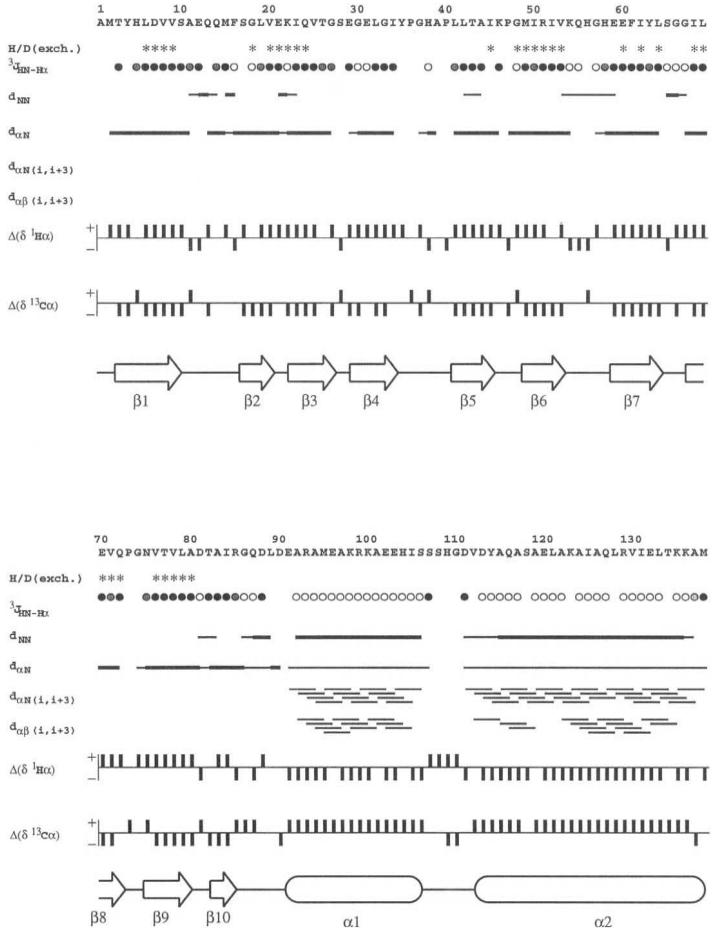

Fig. 1 A summary of spectral data used to identify the secondary structure of the ε subunit. Sequential and medium-range NOE connectivities from the 3D ^{15}N-NOESY-HSMQC and 3D ^{13}C/^{15}N-NOESY-HSQC are drawn by horizontal lines with thick lines indicating strong and thin lines medium to weak NOE cross peaks; slowly exchanging amides are marked with a star if the amide proton was still present after 15 min in D_2O buffer at 22 °C and pH 7.4 (uncorrected). These amides were considered as a hydrogen bond donor; Vicinal $^3J_{HN\text{-}H\alpha}$-coupling constants are indicated by filled circles (J > 7Hz), shaded circles (6Hz < J < 7Hz) or empty circles (J < 6Hz). The absence of a circle indicates that data could not be obtained due to spectral overlap or exchange broadening of the corresponding amide proton. Chemical shift deviations of the ^{13}Cα carbon and α-proton from the corresponding random coil values according to the chemical shift index algorithm (CSI)[42]. A chemical shift index of +1 or -1 is drawn if the chemical shift deviation of the Hα is larger than 0.1 p.p.m. down- or upfield, respectively. The corresponding values for the ^{13}Cα are +0.5 and -0.8, respectively. The bottom of the diagram shows a schematic assignment of the secondary structure of the ε subunit based on the spectral data. Arrows indicate β-strands and cylinders represent α-helices.

nance assignments were obtained from a 3D (CCO)TOCSY-NH experiment.

Secondary structure elements in the ε subunit were identified from characteristic sequential and medium range NOE connectivities,vicinal $^3J_{HN\text{-}H\alpha}$-coupling constants, and the observed deviations of the α-carbon and α-proton chemical shifts from the corresponding random coil values. Hydrogen/deuterium exchange kinetics were also used to establish secondary structure based on hydrogen-bonding patterns. A summary of these experimental parameters and a schematic assignment of the corresponding secondary structure elements is given in Fig. 1. The amounts of α and β structure based on the NMR data are 31% and 36%, respectively which agrees well with the values of 30% and 26% predicted by the algorithm of Chou and Fasman[17].

Table 1 Structural statistics

	residues 1–90	residues 91–138
total number of NOEs	627	390
intra residue (i=j)	192	104
sequential ($\|i\text{-}j\|$ = 1)	202	168
medium range ($\|i\text{-}j\|$ < 5)	26	101
long range ($\|i\text{-}j\|$ > 4)	165	17
hydrogen bonds	21	—
backbone ϕ-angles[1]	41	38
r.m.s.d. (backbone)[2]	1.7 Å	2.1 Å
r.m.s.d. (non-H atoms)[2]	2.4 Å	2.9 Å

[1]Backbone ϕ-angles were restrained to -140°±40° (β-sheet) and -60°±40° (α-helix).
[2]For the average, minimized structure of the 20 lowest energy structures out of a pool of 60 structures for the β-domain and for the average, minimized structure of the eight lowest energy structures out of a pool of 20 structures for the α-domain.

The global fold of the ε subunit

The secondary structure assignments and subsequent analyses indicated that the ε subunit is organized in two domains. To facilitate analysis of the global fold of this polypeptide, the two domains were initially analyzed separately. A tertiary fold was calculated for the 90 N-terminal residues using a total of 585 unambiguous NOE-based distance restraints including 192 intra-residue, 202 sequential (i-j = 1), 26 medium-range (i-j < 5) and 165 long range (i-j > 4) NOEs. A total of 41 backbone ϕ-angle restraints were also included (summarized in Table 1). A starting pool of 60 embedded structures was created with distance geometry and refined by simulated annealing protocols until stable. An average structure was then calculated from the 20 lowest energy structures and subjected to minimization using standard bond lengths and angles. This average structure was then used to search for the hydrogen-bond acceptors from the corresponding slowly exchanging amides. As a result, 21 hydrogen bonds were included as additional distance restraints, and the refinement of all 60 structures was repeated. The final average structure was calculated from the 20 lowest energy structures with no

NOE violations greater than 0.5 Å and no backbone ϕ-angle violations greater than 5°.

Fig. 2*a* shows an overlay of the 10 structures with the lowest backbone r.m.s. deviations to the mean structure, aligned for optimum overlap of the backbone atoms while Fig. 2*b* shows the final average for the structure of the N-terminal domain of the ε subunit in two different orientations. The r.m.s. deviations for the backbone atoms for the 20 structures used to calculate the average structure is 1.7 Å. The arrangement of the C-terminal 48 residues has been determined so far from a total of 340 backbone ϕ angle restraints (Table 1). No slowly exchanging amide protons could be observed for residues 91–138 at pH 7.4.

The N-terminal domain including residues 3-90 is a 10-stranded β-structure which folds as a flattened β-barrel or β-'sandwich'. The 10 β-strands are arranged in roughly two layers, one composed of strands 2,1,9,8,5 and the second involving strands 4,3,6,7,10. All of the β-strands are paired in an antiparallel fashion, with the exception of β1(His 5–Ser 10) and β9(Asn 75–Ala 80) which are aligned parallel to one another as shown in Fig. 2*b*. The interior of the structure is composed almost exclusively of hydrophobic residues including Leu 6, Val 8, Val 20, Ile 23, Val 25, Leu 32, Ile 34, Ile 50, Ile 52, Ile 62, Leu 64, Leu 69, Val 71, Val 76 and Val 78.

The C-terminal part of the ε subunit from residue Glu 91 is folded in two α-helices running antiparallel to each other linked by a loop formed by residues Ser 107 to Asp 111. This part of the ε subunit is currently less well defined than the more interesting N-terminal domain. However, long-range NOEs between residues Ala 92, Ala 94, Lys 98, Glu 102 and Ile 105 of the first helix and residues Ile 131, Leu 128, Ile 125, Leu 121 and Tyr 114 of the second helix indicate that the two α-helices lie close together for their entire length.

Interaction between N- and C-terminal domains

Only a few NOEs have been identified that position the N- and C-terminal domains relative to one another. Therefore we found alternative approaches to finding contact points between two domains using nitroxide spin labelling of two mutants of the ε subunit. Nitroxide spin labels are known to broaden (quench) any NMR signal within a sphere of approximately 10–15 Å radius of the unpaired electron. This line-broadening (induced by either paramagnetic ions or organic radicals bound to the protein) is the basis for the paramagnetic diffrence spectrum technique (PD), originally developed to facilitate spectral analysis of crowded 1D ^{1}H-spectra of proteins[18] (for an overview see ref. 19). More recently, the technique has been used as a tool for structural analysis of proteins by 2D homonuclear NMR, for example in the structure determination of the *c* subunit of the F_0 part of the F_1F_0 ATP synthase from *E. coli*[20]. For the spin labelling, we used two mutants of the ε subunit with cysteine residues introduced at position 10 or 108, respectively, which were used as sites of covalent attachment of the nitroxide (TEMPO maleimide). A qualitative comparison of corresponding peak volumes in ^{1}H-^{15}N correlation spectra, recorded before and after reduction of the nitroxide, identify residues close to the sites of nitroxide incorporation. Fig. 3 shows sample data for the nitroxide modified mutant ε S10C.

Nitroxide modification of ε S10C leads to a complete quenching of the NMR signals from residues Tyr 63–Gly 66 and from residues between Ala 80–Asp 90, thereby confirming the tertiary fold calculated from the NOE input data. Also affected were residues between Lys 123 and Val 130, which means that

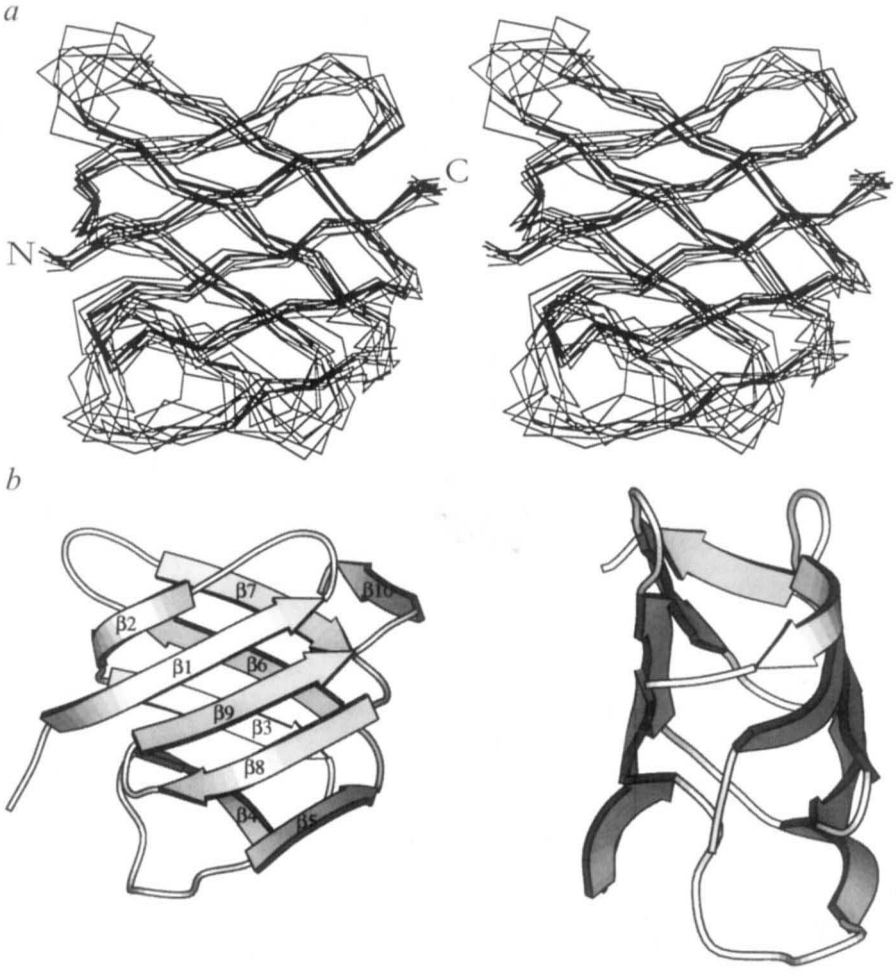

Fig. 2 *a*, Stereoview of an overlay of the backbones for the 10 lowest energy structures for the N-terminal domain of the ε subunit (residues 3–86). The structures are aligned for optimum overlap of the backbone atoms. *b*, Ribbon diagram of the tertiary fold of the N-terminal domain of the ε subunit (two views). The presented structure is an average calculated from the 20 lowest energy structures. The diagrams have been generated in MOLSCRIPT[43].

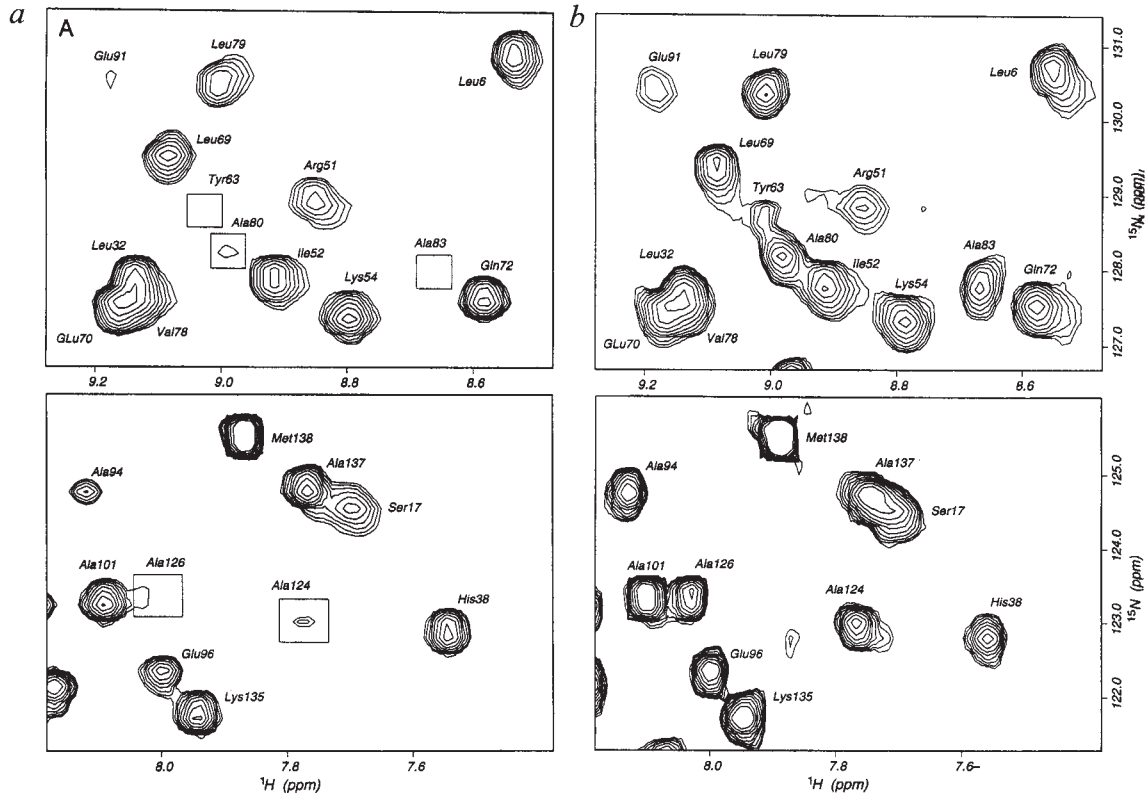

Fig. 3 NMR spectral analysis of the ε subunit modified with TEMPO at position 10. *a*, Two regions from a ^{1}H- ^{15}N-HSMQC spectrum of TEMPO- modified εS10C. *b*, The same regions of a spectrum taken after the spin label had been reduced to the corresponding *N*-hydroxy-amine with sodium dithionite. Residues which are affected by the nitroxide spin label are surrounded by rectangles.

the second helix from Val 112 to Met 138 folds back to the β-sandwich near the end of β-strand 1. Fig. 4 gives a summary of the spin label data for the mutant ε S10C and the proposed arrangement of the C-terminal two-helix hairpin with respect to the N-terminal β-structure. TEMPO-modification of Cys 108, in turn, completely quenched the NMR signals from residues between Glu 102 and Leu 121 in the C-terminal domain. However, little or no quenching of any parts of the N-terminal domain was observed, indicating that the loop region between the two helices is distant from the β-sheet domain.

The spin label data are consistent with the few long-range NOEs so far identified between the side chains of Ala 126, Gln 127 and Thr 134 of the C-terminal α-helix and Tyr 63 and Phe 61 of the N-terminal β- domain. These side chains together with Ile 131 and Leu 133 form a hydrophobic cluster which comprises part of the contact site of the N-terminal and C-terminal domain. It must be remembered that this interaction between the two domains is for isolated ε subunit and a different arrangement or conformationally sensitive arrangements could occur when ε is part of the F_1F_0–ATP synthase complex.

Correlation of genetic and NMR data

The two-domain structure of the ε subunit had been expected based on genetic studies[21] which showed that a mutant of the ε subunit containing only residues 1–80 (but with three additional residues from the cloning vector attached at the C-terminus)—here shown to be the N-terminal β-barrel domain—was capable of forming an active ECF_1F_0. A construct containing only residues 1–73, which would remove β-strands 9 and 10, failed to form a membrane-bound F_1-ATPase. Instead ATPase activity was found in the cytosol.

In subsequent studies, Jounouchi *et al.*[22] found that ECF1 containing an ε subunit lacking the N-terminal 15 amino acids could bind to F_0 to form a functionally active enzyme, a deletion which would remove, approximately, β-strand 1. However, the removal of residue Phe 16 in the construct Ser 17-Met 138 resulted in defective coupling of ATP hydrolysis or synthesis in catalytic sites to proton translocation through F_0. Phe 16 is roughly at the beginning of β-strand 2. Jounouchi *et al.*[22] also showed that an ε subunit mutant missing the ^{15}N-terminal residues, and as few as four residues from the C-terminus, was defective in oxidative phosphorylation. Based on the spin labelling data, the C-terminal part and the end of β-strand 1 are in contact in the region around Gln 127 and Ser 10, respectively. Therefore the C-terminal α-helix domain, by interacting with one end of the β-sheet sandwich, may stabilize the overall N-terminal domain when β-strand 1 is missing.

Position of the ε subunit in the complex

Correlation of the structure of the ε subunit described here with several recently reported cross-linking studies provides the orientation of this subunit in the ECF_1F_0 complex (Fig. 5). The C-terminal two-helix hairpin provides the contact of the ε subunit with the α and β subunits of the F_1 part. Thus a zero-length cross-link can be formed between Ser 108 of ε and Glu 391 of the β subunit (in the so called DELSEED region of the β subunit) by the water-soluble carbodiimide EDC[23,24]. Additionally, a disulphide bond can be generated between a Cys substituted at position 108 of ε and a Cys replacing Glu 381 of the β-subunit[25]. This disulphide bond inhibits ATPase activity of the enzyme, which is fully restored when the bond is broken with reducing agents. A disulphide bond can also be formed between Cys 108 of ε and a Cys at residue 411 of the α-subunit (Aggeler, R. and Capaldi, R. A., unpublished results). The structure of MF_1 (ref. 6) shows a similar fold of α-and β-subunits with residue α-411 being the equivalent of β-Glu 381.

There is genetic evidence, and more recently biochemical evidence, that a region of the ε subunit including Glu 31 and His 38 interacts with the F_0 part. Thus a mutant in the loop region of subunit c of the F_0, E42Q, is suppressed by a change of Glu 31 to Gly, Val or Lys in the ε subunit[26]. A His to Cys mutation at position 38 of the ε subunit has no effect on enzyme functioning[27]. However, NEM (N-ethylmaleimide) modification of this Cys uncouples ATP hydrolysis from proton translocation[28]. Moreover, the Cys at position 38 is readily reactive with a variety of maleimides in isolated ECF_1, but this site is blocked in ECF_1F_0 (ref. 28) indicating its proximity to the F_0 portion. In the structure determination, both Glu 31 and His 38 are at the opposite 'end' of the β-structure from the C-terminal two-helix hairpin (Fig. 5). As the 10-stranded β-barrel is maximally 27 Å in dimension, the helix hairpin must be tilted relative to the N-terminal domain, and extend some 10–15 Å in order to make it possible for the ε subunit to span the distance of 40–45 Å from the F_0 to the α and β subunits estimated by electron microscopy measurements of the stalk in the ECF_1F_0 complex[4,5].

The other major interaction of the ε subunit in ECF_1 is with the γ subunit. Evidence has recently been obtained from cross-linking studies that Ser 10 (ref. 12) and Thr 43 (Tang, C. and Capaldi, R.A., manuscript in preparation) are close to the γ subunit interface. As shown in Fig. 5, these residues are on the face of the β-sheet formed by strands 2,1,9,8,5 and are close to a contiguous hydrophobic patch, or stripe, provided by the side chains of Val 9, Met 15, Leu 42, Ile 68, Thr 77 and Leu 79. These residues, therefore, may contribute to the interaction with the γ subunit.

Functional implications

The ε subunit has several functions in the ECF_1F_0 complex. It is a structural element, as removal or truncation of the subunit affects the binding of the F_1 to the F_0 part[7,21]. In isolated ECF_1 (refs 8,9) and to a lesser extent in ECF_1F_0 (ref. 10), the ε subunit acts as an inhibitor. Removal of this subunit from isolated ECF_1 increases ATPase activity as much as 10-fold. Conversion of Ser 10 to a Cys by itself is sufficient to activate ECF_1 twofold, while reaction of this Cys with bulky maleimides causes loss of the inhibitory function of the ε subunit. Modification of a Cys introduced at Thr 43 with fluorescein-maleimide likewise affects the inhibitory properties of the ε subunit (Tang, C. and Capaldi, R. A., manuscript in preparation), suggesting that interaction of this subunit with the γ subunit plays a role in modulating ATPase activity. Kuki *et al.*[21] found that a truncated ε subunit containing residues 1–93 (plus two serine residues from the plasmid) retained partial inhibitory function while the construct of residues 1–80 had completely lost this inhibitory activity. These findings can be explained if removal of β-strand 10 disrupts the γ subunit binding face while still allowing overall folding of ε. Trypsin treatment to remove part of the C-terminal domain also causes a loss of inhibitory function of the ε subunit. How this occurs is not clear from the structural data.

A second function of the ε subunit is in coupling of catalytic-site events in the F_1 part with proton translocation through the F_0 part. This energy coupling is known to involve conformational changes including translocations of the ε subunit, as well as the γ subunit,

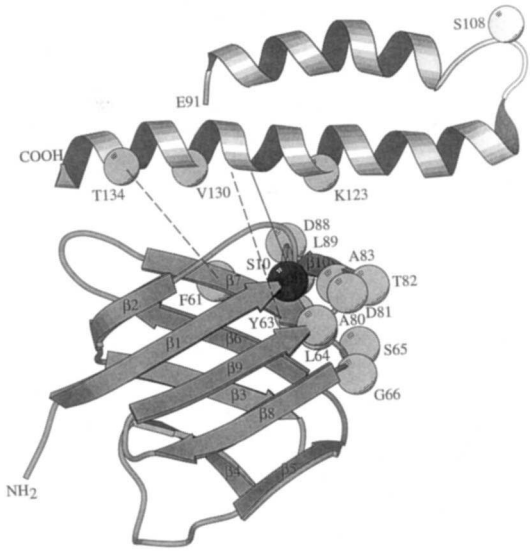

Fig. 4 Interaction of the N-terminal β-structure with the C-terminal two-helix hairpin based on spin label perturbation of NMR spectra and unambiguous long-range NOEs. The N-terminal domain is the average of the 20 lowest energy structures as already shown in Fig. 2*b*. The C-terminal domain is the best structure out of a pool of 20 initial structures. Residues which are perturbed by a TEMPO spin label attached at residue Cys 10 in the mutant ε S10C are shown with space filling α-carbons in light grey. The quenching of the NMR signal of residues between Lys 123 and Val 130 from the spin label bound to position 10 is indicated by a solid line. Long-range NOEs could be identified between residues Phe 61 and Tyr 63 of the N-terminal domain and residues Thr 134 and Gln 127 in the C-terminal α-helix (broken lines). The figure was generated using MOLSCRIPT[43].

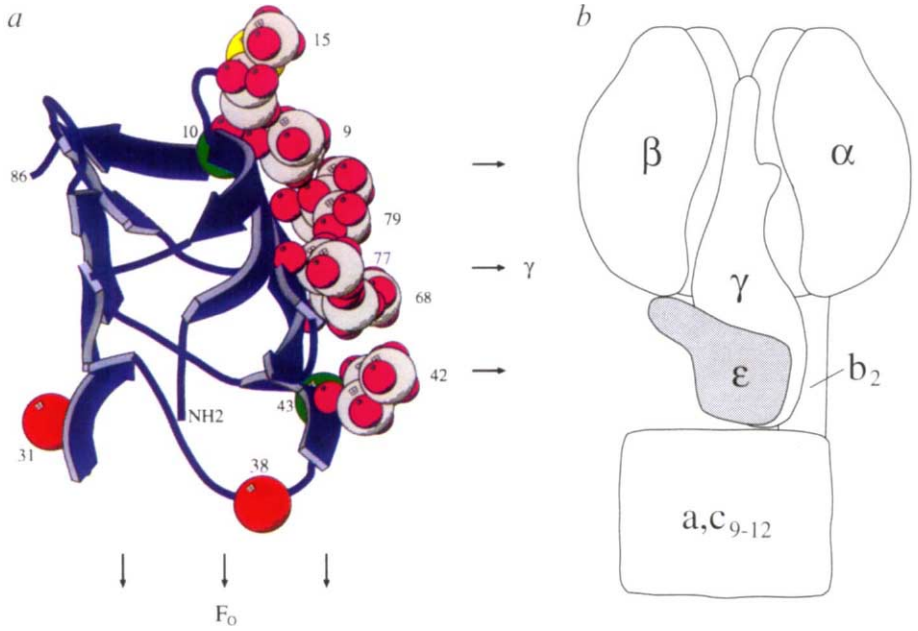

Fig. 5 Arrangement of the ε subunit in the ECF_1F_0 complex. *a*, The ε subunit is seen oriented 90° relative to that shown in Fig. 4, thus presenting a view parallel to the two layers of the 'sandwich'.The side chains of the hydrophobic residues Val 9, Met 15, Leu 42, Ile 68, Thr 77 and Leu 79 are shown with hydrogen in pink and carbon in light grey. Ser 10, Glu 31, His 38 and Thr 43 are indicated by the position of the corresponding α-carbon atoms. The orientation of the ε subunit, based on cross-linking and genetic studies (see text for details), is indicated by arrows pointing to the corresponding site of interaction in the F_1F_0 complex. Contacts to F_1 are mediated by the C-terminal two-helix hairpin, which in turn lies near residue 10 of the ε subunit. Contacts to F_0 involve residues 31 and 38 (shown in red). The interface to the γ subunit may involve the hydrophobic residues along one face of the β-sandwich of ε. *b,* Schematic representation of the arrangement of the ε subunit in the ATP synthase complex (one αβ pair and the δ subunit are not shown). The size and the asymmetric location of the ε subunit gives the stalk a wider appearance with dimensions slightly bigger than the dimensions obtained by cryo-electron microscopy[4]. The value of the diameter of the stalk measured from averages of single molecule projections of ice-embedded F_1F_0 complexes is probably underestimated since the single molecules used for averaging likely have different orientations with respect to an axis perpendicular to the membrane bilayer. As a result, any asymmetric density within the stalk would be averaged out.

within the ECF_1F_0 complex (reviewed in ref. 15). The structural features reported here suggest an additional aspect to this coupling function of the ε subunit. The structural motif found in the N-terminal domain of the ε subunit, a 10-stranded β-sandwich or flattened barrel, has been found for a number of other proteins all involved in binding hydrophobic compounds (the lipid- or fatty acid- binding proteins; for a review on this class of proteins, see ref. 29). This raises the possibility that the ε subunit also binds fatty acids or lipid molecules, which could regulate F_1F_0 function, or more intriguingly, could be proton carriers across the F_0 (to and from the ε subunit) instead of there being a proton wire, as usually speculated[1-3].

Methods

^{13}C ^{15}N-labelled ε subunit. The ε subunit of the *E. coli* F_1F_0 ATP synthase was produced using a bacterial expression system according to Patel *et al*[30] Uniformly ^{15}N or $^{13}C/$ ^{15}N-labelled protein was biosynthetically prepared using *E. coli* strains K38 or 594 (ref.31) grown in M9T minimal medium with 99 % ^{13}C 6-glucose and $(^{15}NH_4)_2SO_4$ (Isotec, Inc.) as the sole carbon- and nitrogen sources, respectively. Selectively ^{15}N-labelled ε subunit was obtained by expression in *E. coli* strains D446 and DL39 grown in a synthetic rich medium containing either ^{15}N-labelled alanine, valine, leucine, ioleucine or glutamic acid[31]. N-terminal sequencing of the purified ε subunit revealed that the N-terminal Met is posttranslationally removed *in vivo*, the numbering system used in this study therefore starts with Ala at position 1. Protein concentrations were determined by UV absorbance at 277 *nm*, using a calculated extinction coefficient of 5800 mol^{-1} cm^{-1} (ref. 32). The homogenity of protein samples was confirmed by SDS-polyacrylamide gel electrophoresis. Based on equilibrium centrifugation, the ε subunit behaves as a monomeric species up to the highest concentration tested (4.5 mg ml^{-1}). The proton linewidth measured with NMR samples is also consistent with a monomeric protein of relative molecular mass 15,000.

TEMPO-modification of ε mutants S10C and S108C. Uniformly ^{15}N-labelled ε subunit with a site-directed cysteine on position 10 or 108 (ref. 12) was reacted at a concentration of 0.8-1.0 mM with a fourfold molar excess of TEMPO-maleimide (Sigma) in 5 mM potassium phosphate (pH 7.4), 0.1 mM EDTA and 0.5 mM DTT. After 1 hr at room temperature, excess label was removed by two consecutive passes through Sephadex G25 (SIGMA) spin columns in the above buffer without DTT and EDTA. Spectra were recorded before and after reduction of the nitroxide with a twofold molar excess of sodium dithionite[33].

NMR spectroscopy. All NMR spectra of unlabelled and ^{15}N labelled protein samples were recorded on a General Electric GN 500 spectrometer (F.W.D.) operating at 11.7 T. Experiments involving ^{13}C-labelled protein were performed on a Varian Unity 500 spectrometer equipped with a pulsed field gradient accessory (L.P.M). Protein samples were between 0.6 and 1 mM (9–15 mg ml^{-1}) in 5 mM potassium phosphate buffer (pH 7.4), 100 mM D_6-DMSO, 3 mM NaN_3 and 5% D_2O. Spectra were recorded at 18–22 °C.

The following NMR experiments were used in this study: 2D ^{15}N-^1H HSMQC with either presaturation or a jump-return sequence for water suppression[34], 3D ^{15}N-edited NOESY-HSMQC (mixing time 100 ms) and 3D ^{15}N-TOCSY-HSMQC[35,36] sensitivity-enhanced 3D C(CO)NH and H(CCO)NH (ref. 37) and simultaneous $^{15}N^{13}C$ resolved NOESY[38]. Aromatic resonances were assigned from 2D DQF-COSY and TOCSY experiments recorded in D_2O, and ((Hβ)CβCγCδ)Hδ and (Hβ)Cβ(CγCδCε)Hε experiments recorded in H_2O (ref. 39). NOE-based distance restraints were also collected from a 2D NOESY spectrum recorded in D_2O. Vicinal $^3J_{HN\text{-}H\alpha}$ -coupling constants were determined from a series of eight 2D-J-modulated HSQC experiments[40]. Hydrogen/deuterium exchange rates were measured after dissolving lyophilized uniformly ^{15}N-labelled ε subunit in 99.9% D_2O (Cambridge Isotopes) followed by a series of ^1H-^{15}N-HSMQC experiments. Full details of the NMR data collection and analysis will be

presented elsewhere. All structure calculations were performed with the program X-PLOR[41] following standard protocols. First, a template structure with ideal local geometry was created. This template structure was then used to calculate a pool of embedded structures using distance geometry. The embedded structures were regularized and repeatedly refined by distance geometry and simulated annealing. The coordinates of the final structures for the two domains of the ε subunit will be deposited in the Brookhaven protein databank.

Received 5 July; accepted 21 August 1995.

Acknowledgements
This work was supported by National Institutes of Health Grant (R.A.C), a grant from the Markey Foundation (R.A.C and F.W.D) and instrument support from the Canadian Protein Engineering Network of Centres of Excellence (L.P.M).

1. Senior, A. ATP synthesis by oxidative phosphorylation. *Physiological Reviews* **68**, 177–231 (1988).
2. Futai, M., Noumi, T. & Maeda, M. ATP synthase (H+-ATPase): Results by combined biochemical and molecular biological approaches. *A. Rev. Biochem.* **58**, 111–136 (1989).
3. Penefsky, H. & Cross, R.L. Structure and mechanism of F_1F_0 ATP synthases and ATPases. *Adv. Enzymol.* **64**, 173–214 (1991).
4. Gogol, E.P., Lucken, U. & Capaldi, R.A. The stalk connecting the F_1 and F_0 domains of ATP synthase visualized by electron microscopy of unstained specimens. *FEBS Lett.* **219**, 274–278 (1987).
5. Lücken, U., Gogol, E.P. & Capaldi, R.A. Structure of the ATP synthase complex (ECF_1F_0) of *Escherichia coli* from cryoelectron microscopy. *Biochemistry* **29**, 5339–5343 (1990).
6. Abrahams, J. P., Leslie, A.G.W., Lutter, R. & Walker, J.E. Structure at 2.8 Å resolution of F_1-ATPase from bovine heart mitochondria. *Nature* **370**, 621–628 (1994).
7. Sternweis, P.C. & Smith, J.B. Characterization of the purified membrane attachment β-subunit of the proton translocating ATPase from *Escherichia coli*. *Biochemistry* **16**, 4020–4025 (1977).
8. Sternweis, P.C. & Smith, J.B. Characterisation of the inhibitory ε subunit of the proton-translocating ATPase from *Escherichia coli*. *Biochemistry* **19**, 526–531 (1980).
9. Mendel-Hartvig, J. & Capaldi, R.A. Catalytic site nucleotide and inorganic phosphate dependence of the conformation of the ε subunit in *Escherichia coli* adenosinetriphosphatase. *Biochemistry* **30**, 1278–1284 (1991).
10. Mendel-Hartvig, J. & Capaldi, R.A. Nucleotide-dependant and dicyclohexylcarbodimide-sensitive conformational changes in the ε subunit of *Escherichia coli* ATP synthase. *Biochemistry* **30**, 10987–10991 (1991).
11. Turina, P. & Capaldi, R.A. ATP hydrolysis-driven structural changes in the γ-subunit of *Escherichia coli* ATPase monitored by fluorescence from probes bound at introduced cysteine residues. *J. Biol. Chem.* **269**, 13465–13471 (1994).
12. Aggeler, R., Chicas-Cruz, K., Cai, S.-X., Keana, J.F.W. & Capaldi, R.A. Introduction of reactive cysteine residues in the ε subunit of *Escherichia coli* F_1 ATPase, modification of these sites with tetrafluorophenyl azide-maleimides and examination of changes in the binding of the ε subunit when different nucleotides are in catalytic sites. *Biochemistry* **31**, 2956–2961 (1992).
13. Gogol, E.P., Johnston, E., Aggeler, R., & Capaldi, R.A. Ligand-dependant structural variations in *Escherichia coli* F_1-ATPase revealed by cryoelectron microscopy. *Proc. natn. Acad. Sci. U.S.A.* **87**, 9585–9589 (1990).
14. Wilkens, S. & Capaldi, R.A. Asymmetry and structural changes in ECF_1 examined by cryoelectronmicroscopy. *Biol. Chemistry Hoppe-Seyler* **375**, 43–51 (1994).
15. Capaldi, R.A., Aggeler, R., Turina, P. & Wilkens, S.Coupling between the catalytic sites and the proton channel in F_1F_0-type ATPases. *TIBS* **219**, 284–289 (1994).
16. Bianchet, M., Ysern, X., Hullihen, J., Pedersen, P.L. & Amzel, L.M. Mitochondrial ATP synthase: Quaternary structure of the F_1 moiety at 3.6 Å determined by x-ray diffraction analysis. *J. biol. Chem.* **266**, 21197–21201 (1991).
17. Chou, P. Y. & Fasman, G. D. Prediction of the secondary structure of proteins from their amino acid sequence. *Adv. Enzymol. Relat. Areas molec. Biol.* **47**, 45–148 (1978).
18. Campbell, I.D., Dobson, C.M., Williams, R.J.P. & Xavier, A.V. Resolution enhancement of protein PMR spectra using the difference between a broadened and a normal spectrum. *J. magn. Reson.* **11**, 172–181 (1973).
19. Kosen, P.A. Spin labeling of proteins. *Meths Enzymol.* **177**, 86–121 (1989).
20. Girvin, M.E. & Fillingame, R.H. Determination of local protein structure by spin label difference 2D NMR: The region neighboring Asp61 of subunit c of the F_1F_0 ATP synthase. *Biochemistry* **34**, 1635–1645 (1995).
21. Kuki, M., Noumi, T., Maeda, M., Amemura, A. & Futai, M. Functional domains of ε subunit of *Escherichia coli* H+-ATPase (F_1F_0). *J. biol Chem.* **263**, 17437–17442 (1988).
22. Jounouchi, M., Takeyama, M., Noumi, T., Moriyama, Y., Maeda, M. & Futai, M. Role of the amino terminal region of the ε subunit of *Escherichia coli* H+-ATPase (F_0F_1). *Arch. Biochem. Biophys.* **292**, 87–94 (1992).
23. Lötscher, H.-R., deJong, C. & Capaldi, R.A. Inhibition of the ATPase activity of *Escherichia coli* F_1 by the water-soluble carbodiimide1-ethyl-3-[3(dimethylamino)propyl]carbodiimide is due to modification of several carboxyls in the β subunit. *Biochemistry* **23**, 4134–4140 (1984).
24. Dallmann, H.G., Flynn, T.G. & Dunn, S.D. Determination of the 1-ethyl-3-[3(dimethylamino)propyl] carbodiimide induced cross-link between the β & ε subunits of *Escherichia coli* F_1-ATPase. *J. biol. Chem.* **267**, 18953–18960 (1992).
25. Aggeler, R., Haughton, M.A. & Capaldi, R.A. Disulfide bond formation between the COOH-terminal domain of the β subunits and the γ and ε subunits of the *Escherichia coli* F_1-ATPase. *J. biol. Chem.* **270**, 9185–9191 (1995).
26. Zhang, Y., Oldenburg, M. & Fillingame, R. Suppressor mutations in F_1 subunit ε recouple ATP-driven H+ translocation in uncoupled Q42E subunit *c* mutant of *Escherichia coli* F_1F_0 ATP synthase. *J. biol. Chem.* **269**, 10221–10224 (1994).
27. Skakoon, E.N. & Dunn, S.D.Location of conserved residue histidine-38 of the ε subunit of *Escherichia coli* ATP synthase. *Arch. Biochem. Biophys.* **302**, 272–278 (1993).
28. Aggeler, R., Weinreich, F. & Capaldi, R.A. Arrangement of the ε subunit in the *Escherichia coli* ATP synthase from the reactivity of cysteine residues introduced at different positions in this subunit. *Biochem. Biophys. Acta.* **1230**, 62–68 (1995).
29. LaLonde, J.M., Bernlohr, D.A. & Banaszak, L.J. The up-and-down β-barrel proteins. *FASEB J.* **8**, 1240–1247 (1994).
30. Patel, H.-G. Dallmann, H.G., Skakoon, E.N. Kapala, T.D. & Dunn,S.D. The *Escherichia coli unc* transcription terminator enhances expression of *uncc*, encoding the ε subunit of F_1-ATPase, from plasmids by stabilizing the transcript. *Molec. Microbiol.* **4**, 1941–1946 (1990).
31. Muchmore, D.C., McIntosh, L.P., Russel, C.B., Anderson, E.D. & Dahlquist, F.W. Expression and ^{15}N-labeling of proteins for proton and ^{15}N NMR. *Meths Enzymol.* **177**, 44–73 (1989).
32. Gill, S.C. & von Hippel, P.H. Calculation of protein extinction coefficients from amino acid sequence data. *Anal. Biochem.* **182**, 319–326 (1989).
33. Ozinskas, A.J. & Bobst, A.M. Formation of NV-hydroxy-amines of spin labeled nucleosides for ^1H-NMR analysis. *Helv. Chim. Acta* **63**, 1407–1411 (1980).
34. Zuiderweg, E.R.P. A proton-detected heteronuclear chemical-shift correlation experiment with improved resolution and sensitivity. *J. Magn. Reson.* **86**, 346–357 (1990).
35. Zuiderweg, E.R.P. & Fesik, S.W. Heteronuclear three-dimensional NMR spectroscopy of the inflammatory protein C5a. *Biochemistry* **28**, 2387–2391 (1989).
36. Marion, D., Kay, L.E., Sparks, S.W., Torchia, D.A. & Bax, A. Three-dimensional heteronuclear NMR of ^{15}N-labeled proteins. *J. Am. Chem. Soc.* **111**, 1515–1517 (1989).
37. Grzesiek, S., Anglister, J. & Bax, A. Correlation of backbone amide and aliphatic side-chain resonances in $^{13}C^{15}N$-enriched proteins by isotropic mixing of ^{13}C magnetization. *J. Magn. Reson. Series B* **101**, 114–119 (1993).
38. Pascal, S.M., Muhandiram, D.R., Yamazaki, T., Forman-Kay, J.D. & Kay, L.E. Simultanous acquisition of $^{15}N/^{13}C$-edited NOE spectra of proteins dissolved in H_2O. *J. magn. Reson. Series B* **103**, 197–201 (1994).
39. Yamazaki, T., Forman-Kay, J.D. & Kay, L.E. Two-dimensional NMR experiments for collecting $^{13}C\beta$ & $^1H\delta/\epsilon$ chemical shifts of aromatic residues in ^{13}C-labelled proteins via selective couplings. *J. Am. Chem. Soc.* **115**, 11054–11055 (1994).
40. Billeter, M., Neri, W.D., Otting, G., Qian, Y.Q. & Wüterich, K. Precise vicinal coupling constants $^3N_{HN-\alpha}$ in proteins from nonlinear fits of *JN*-modulated $^{15}N,^1H$)-COSY experiments. *J. biomolec. NMR* **2**, 257–274 (1992).
41. Brünger, A. X-PLOR, version 3.1: A system for X-ray crystallography and NMR. Yale University Press, New Haven, CT. (1992).
42. Wishart, D.S. & Sykes, B.D. Chemical shifts as a tool for structure determination. *Meths Enzymol.* **239**, 363–392 (1994).
43. Kraulis, P.J. MOLSCRIPT: a program to produce both detailed and schematic plots of protein structures. *J. Appl. Crystallogr.* **24**, 946–950 (1991).